Ordering of PS-*b*-P4VP on Patterned Silicon Surfaces

Soojin Park,[†] Bokyung Kim,[†] Ozgur Yavuzcetin,[‡] Mark T. Tuominen,[‡] and Thomas P. Russell[†,*]

[†]Department of Polymer Science & Engineering and [‡]Department of Physics, University of Massachusetts, Amherst, Massachusetts 01003

ABSTRACT We demonstrate a method to fabricate high-quality patterned micelle arrays using poly(styrene-*b*-4-vinylpyridine) (PS-*b*-P4VP) block copolymer. Long-range order of the PS-*b*-P4VP micelle in hexagonal arrays was induced by topographic grating patterns during solvent annealing. The size and row spacing of block copolymer micelle arrays created in this way were uniform. By controlling the thickness of the polymer on the crests and in the troughs of the grating patterns, we prepared PS-*b*-P4VP micelle arrays having different sizes.

KEYWORDS: block copolymer micelle · PS-*b*-P4VP · grating surface · long-range order · Moiré analysis

Highly ordered nanosized features in a confined environment have attracted intense interest owing to their potential applications in optical, optoelectronic, and magnetic devices. The critical issue is the control of their size, spacing, and size distribution.[1–5] Self-assembly is a desirable method for fabricating nanostructured surfaces. In particular, block copolymer systems offer an attractive route for overcoming the limitations of conventional lithographic techniques, owing to their ability to self-assemble into ordered nanoscale morphologies.[6–8] There have been numerous efforts to use self-assembled block copolymers as a tool for fabricating nanomaterials.[9–13]

To achieve high placement accuracy in self-assembled systems, a lithographically prepared template has been used to guide the positions of the self-assembled features. Topographic features of templates on the surfaces, simple edges, or well-defined troughs provide a way for controlling multilevel ordering where a "bottom-up" method such as self-assembly of block copolymers is combined with a "top-down" lithographic method. This method has been applied to numerous systems, including quantum dot formation,[14] arrangement of colloidal spheres,[15] and microphase separation in block copolymers.[16–26] In particular, templating methods in block copolymer systems have successfully generated arrays of spherical,[17,18,20,23] cylindrical,[21,22,24] or lamellar nanostructures[19] with long-range order. Segalman *et al*. reported that substrate topography is efficient in directing long-range order in sphere-forming block copolymers. A monolayer of P2VP spherical microdomains in a poly(styrene-*b*-2-vinylpyridine) (PS-*b*-P2VP) thin film was placed on the photolithographically patterned substrate and was then annealed to generate ordered structures which propagated several micrometers from the side walls of the grooves and the edges of the mesas.[17] Besides 1-D confinement, Hexemer *et al*. created a well-ordered array of PS-*b*-P2VP spheres in a 2-D hexagonal-shaped topographical well with a diagonal width of a few micrometers.[23] Cheng *et al*. investigated various factors affecting the long-range ordering of spherical poly(styrene-*b*-ferrocenyldimethylsilane) between side walls of periodic grooves.[18,20] Recently, Xiao *et al*. demonstrated that chemically modified topographic substrates allow the creation of perpendicularly oriented cylindrical domains in useful architectures with long-range order and regular geometry in thin films of block copolymers.[24]

To control size, spacing, and size distribution of nanostructures, one possible approach is to use block copolymer micelles. In solvents that selectively dissolve only one of the blocks, block copolymers form well-defined micelles with a core consisting of the insoluble block and a shell or corona of the soluble block. These micelles can be spherical, cylindrical, vesicle, or wormlike depending on the block ratios, the interfacial energy between the blocks, and the solvent quality.[27,28] There have been several reports on the preparation of long-range

*Address correspondence to russell@mail.pse.umass.edu.

Received for review November 29, 2007 and accepted May 27, 2008.

Published online June 11, 2008.
10.1021/nn800073f CCC: $40.75

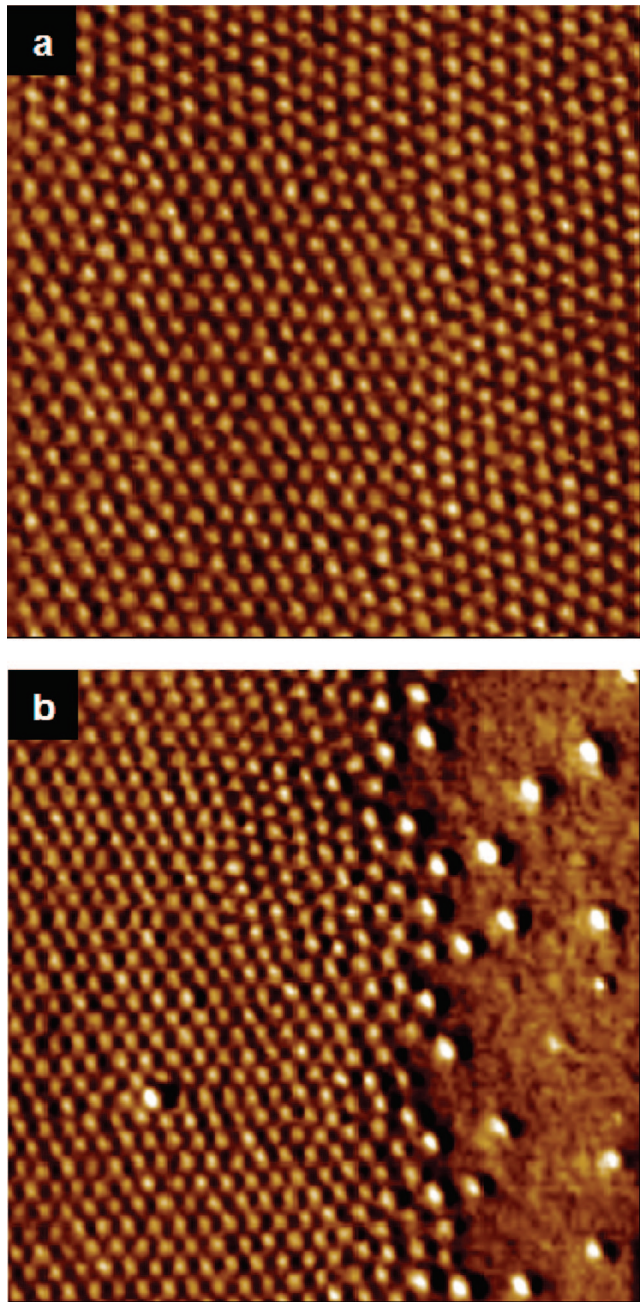

Figure 1. Height mode SFM image (1 μm × 1 μm) of (a) 24 nm thick and (b) 22 nm thick PS-*b*-P4VP films showing the dewetting of PS-*b*-P4VP micelles on a flat surface.

ordered arrays from block copolymer micelles. For example, Xuan *et al*. obtained well-ordered hexagonally packed cylinders in the symmetric copolymer poly(styrene-*b*-methyl methacrylate) thin films by controlling the selectivity of the solvent, film thickness, and the vapor exposure times.[29] Zhao *et al*. investigated the surface morphologies of thin asymmetric poly(styrene-*b*-4-vinylpyridine) (PS-*b*-P4VP) films after solvent annealing in methanol vapor.[30] Recently, Yun *et al*. reported that a near-perfect hexagonal array of block copolymer micelles was created by solvent annealing on a single layer of micelles, which equilibrated the size and positional order of the micelles by redistributing the copolymer chains per micelle.[31]

Here, we demonstrate a new approach for preparing highly ordered arrays of PS-*b*-P4VP block copolymer micelles on a patterned silicon substrate. We studied the time evolution of surface morphologies of PS-*b*-P4VP thin films under solvent vapor. By annealing the PS-*b*-P4VP films in solvent vapor, arrays of PS-*b*-P4VP micelles with a high degree of lateral order are produced. We assess the limiting factors for the micelle arrays having different sizes on the crests and in the troughs of the grating patterns. We also investigated the effect of vapor pressure and crest-to-trough depth on the surface morphologies and lateral order of micelles.

RESULTS AND DISCUSSION

Influence of Grating Width on the Crest-to-Trough Depth of the Polymer Surface. Electron-beam lithography (JEOL 6400 SEM) was used to expose a 100 nm thick film of poly(methyl methacrylate) on oxidized silicon wafers. The single line exposures ranged from 0.3 to 7 nC/cm, which gave different line widths. Development in methyl isobutyl ketone/isopropyl alcohol (1/3, v/v) of the exposed pattern at room temperature for a minute and a rinse in isopropyl alcohol creates troughs with vertical side walls, and the evaporation of 14 nm thick silicon oxide *via* thermal evaporation on the developed region resembles oxidized silicon. This process is followed by acetone lift-off. One-dimensional troughs of various widths were used to study the array of block copolymer micelles. Scanning force microscopy (SFM) was used to measure the representative bare grating pattern of a 100 nm line (see Supporting Information, Figure S1). When PS-*b*-P4VP thin films from 1.2 wt % DMF (Fisher) solution were spin coated onto flat silicon substrates at 2500 rpm for 60 s, the film thickness measured by ellipsometry was 24 nm. When a 24 nm thick layer of PS-*b*-P4VP was spin coated on the grating pattern, the trapezoidal shape is reduced to a sinusoidal modulation with different depths as shown in Figure S2. It should be noted that the separation distances between two crests in all the grating patterns are the same. From the cross sectional scans, we obtained that the crest-to-trough depths of the polymer surface having 120, 100, 80, and 50 nm line widths are 4.3, 3.9, 2.9, and 2.3 nm, respectively (see Supporting Information, Figure S2). It is obvious that the crest-to-trough depth of the polymer surface is somewhat smaller than the respective value of the underlying substrate. This effect is due to the interplay between surface tension and van der Waals interactions, which typically flattens the surface of a polymer film that is deposited onto a pre-existing rough surface.[32–35] Consequently, the film thickness on the crests will be somewhat lower than the thickness in the troughs.

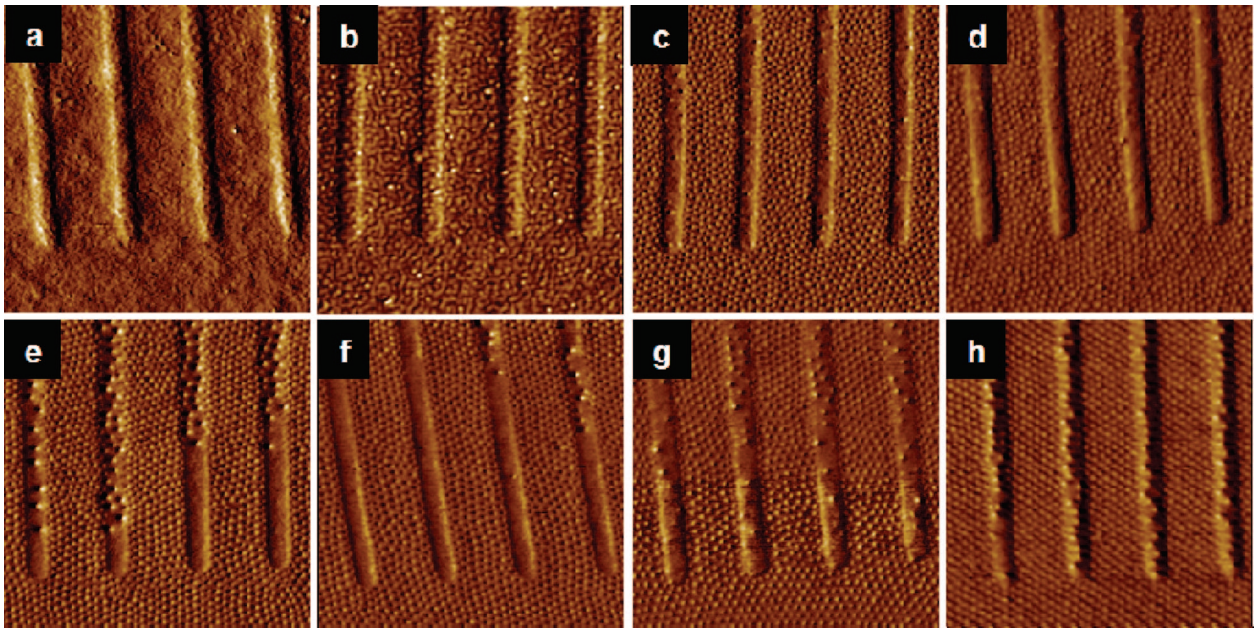

Figure 2. Phase mode SFM images (1.5 μm × 1.5 μm) of PS-*b*-P4VP micellar films developed on the grating width of 100 nm at different annealing times: (a) 5 min, (b) 10 min, (c) 30 min, (d) 1 h, (e) 2 h, (f) 3 h, (g) 4 h, and (h) 6 h.

Time Evolution of Surface Morphologies of PS-*b*-P4VP Films under Solvent Vapor. The PS-*b*-P4VP films were exposed to THF (Fisher) vapor to induce mobility and allow near-perfect hexagonal arrays to occur. To control the solvent vapor treatment process, the samples were kept at a constant temperature (23 °C) in a small closed vessel. It should be noted that THF is a slightly selective solvent for PS, in which micelles were formed upon solvent annealing. The PS blocks form a shell around insoluble P4VP blocks to reduce energetically unfavorable interactions with the solvent.[31] To obtain a monolayer array of PS-*b*-P4VP micelles, the film thickness is the key parameter to control.

Figure 1 shows height mode SFM images obtained from polymer films having a slightly different thickness on flat silicon substrates after solvent annealing in THF vapor for 3 h. Figure 1a shows the well-developed PS-*b*-P4VP micelle arrays without dewetting. In the right-hand side of Figure 1b, one can see that dewetting takes place due to thinness of the polymer film. It should be noted that the PS-*b*-P4VP micelle size near the dewetting regions increased. It appears that isolated micelles near the dewetting regions are unstable in THF vapor and tend to aggregate. To investigate the effect of film thickness on the dewetting phenomena, a 12.8 nm thick layer of PS-*b*-P4VP film was spin coated onto flat silicon substrates, then solvent annealed under the same condition. There was no feature observed in the SFM image, which indicates a wetting layer of PS-*b*-P4VP on the silicon substrate (see Supporting Information, Figure S3). We can expect that P4VP blocks preferentially wet the silicon substrates, as shown in other reports.[36,37]

In the same manner, we studied the time evolution of surface morphologies of PS-*b*-P4VP thin films on grating patterns under THF vapor. Figure 2 shows phase mode SFM images of the films which were annealed from 5 min to 6 h. In the early stage of solvent annealing, dimple type structures of PS-*b*-P4VP were seen randomly (Figure 2a,b). After annealing for 30 min, when the thickness of the polymer film is 1.3 times thicker in vapor, spherical micelles with short-range order were prepared everywhere (Figure 2c). Film thickness in THF vapor reached the saturation point (1.6 times thicker) at 1 h, at which point the order of micelles increases a little bit, as shown in Figure 2d. Until the films were exposed to THF vapor for 4 h, lateral order of micelles increased (Figure 2e−g). In the case of films annealed for 6 h, the lateral order of micelles was dramatically enhanced within grating and edge regions (Figure 2h). However, it still has different orientation at other regions (not shown here), so it requires longer annealing time to increase grain size. From Figure 2, the question concerning the lateral order remains: which region between the inside and outside patterns is better.

The PS-*b*-P4VP films were annealed in THF vapor for 8 h on the grating patterns having different line widths. After annealing, a monolayer of a PS shell around a P4VP core formed within the troughs. The PS-*b*-P4VP micelle arrays in the troughs have an average center-to-center spacing, p, of 43.1 nm and a spacing, d, of 37.2 nm ($d = \sqrt{3}p/2$) between the rows of spherical micelles in a close-packed two-dimensional array. Figure 3 shows the SFM images of highly ordered PS-*b*-P4VP micelle arrays. These indicate that the grating patterns are efficient in promoting long-range order. The differences between micelle arrays in the systems hav-

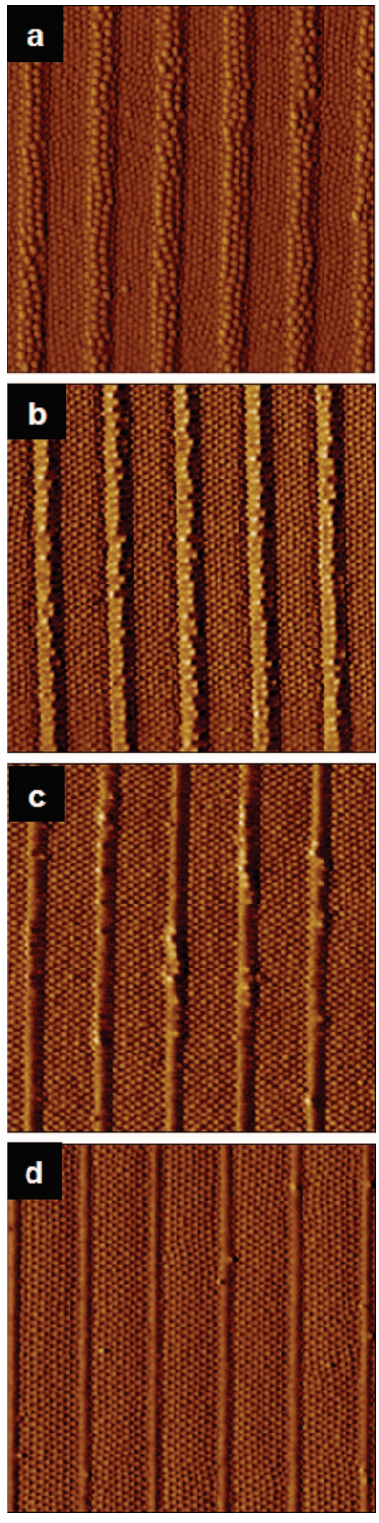

Figure 3. Phase mode SFM images (2 μm × 2 μm) of PS-*b*-P4VP micellar films annealed in THF vapor on grating patterns: (a) 120 nm width, (b) 100 nm width, (c) 80 nm width, and (d) 50 nm width.

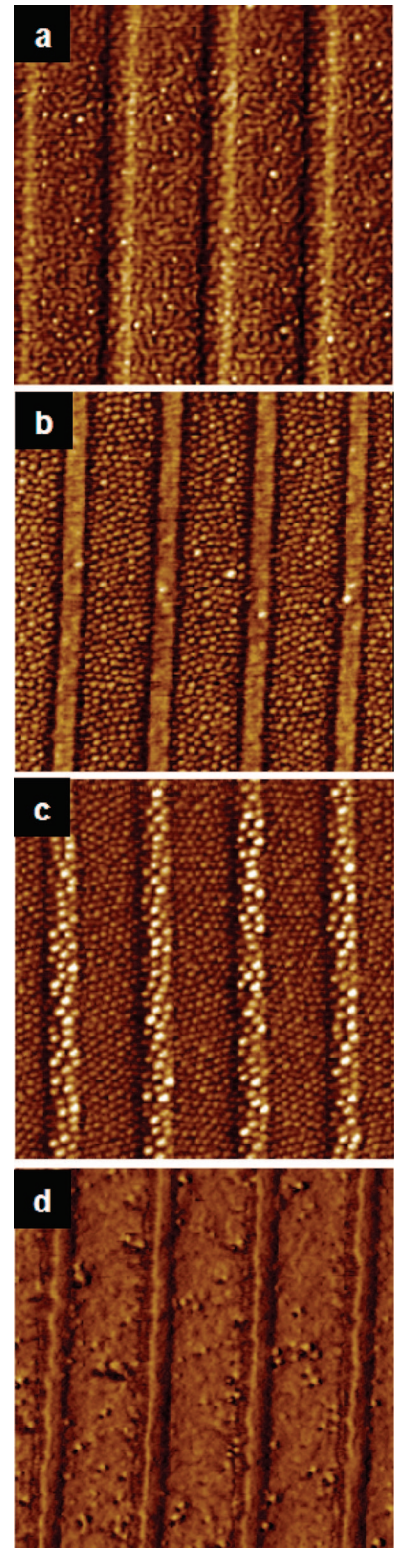

Figure 4. Influence of vapor pressure on the micellar structure of PS-*b*-P4VP films developed on the grating pattern of 100 nm width. Phase mode SFM images of surface morphologies of the thin films annealed for 10 min (a) at 23 °C, (b) 30 °C, and (c) 40 °C. (d) The films developed under additional vapor pressure (1 psi).

ing different line widths are the number of rows and the dewetting on the crests of the grating pattern. The number of rows in the micelle arrays is determined by the trough width (see Supporting Information, Figure S4). The lattice spacing between two micelles in the direction parallel to the trough is equal to the original lattice spacing (d = 37.2 nm) observed on a flat substrate, as shown in Figure 1a. Micelle arrays with N

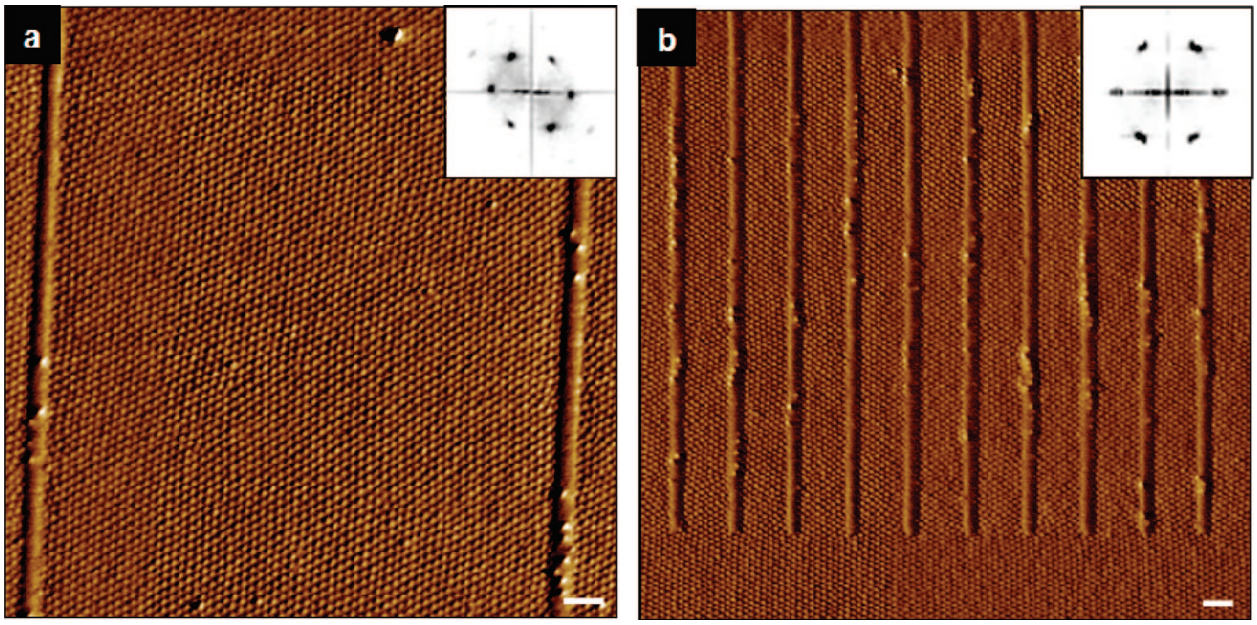

Figure 5. Phase mode SFM images of PS-*b*-P4VP micellar films annealed in THF vapor on a grating width of 2.5 μm (a) and near the grating edge (b). Fourier transforms of panels a and b show the characteristic of the long-range order in the inset. Scale bar = 200 nm.

rows of polymer form for a confinement width W where $(N - 0.5)d < W < (N + 0.5)d$, as shown in Figure S4. When the trough width is incommensurate with the ideal period, d, the periodicity of the block copolymer micelle is compressed or expanded to fit within the trough. These results are in agreement with previous results using the cylinder or sphere-forming block copolymers.[18,20,24]

As mentioned earlier in the spin-coated polymer films, the crest-to-trough depth of the grating pattern of 120 nm line width is 4.3 nm. After solvent annealing, its depth changed from 4.3 to 2.4 nm between the wetting layer on the crest and trough, while the residual polymer, except for the wetting layer, formed larger micelles due to dewetting (see Supporting Information, Figure S5). It appears that the larger micelles on the crests may affect the ordering of the micelle arrays in the trough, as shown in Figure 3a. This problem can be solved by controlling the line width of the grating pattern. As the line width decreases, the crest-to-trough depth of polymer-coated grating patterns is reduced (see Supporting Information, Figure S2). In these cases, smaller amounts of polymer on the crests are left, and after annealing, larger micelles formed in the narrow regions, as shown in Figure 3b,c. This method is effective for preparation of highly ordered micelle arrays having different sizes by controlling the line widths of the grating patterns. When the line width was reduced to 50 nm, only a wetting layer on the crests was seen in the SFM image of Figure 3d. During the spin coating on the grating pattern, a wetting layer of ~12 nm is left on the crest, and larger micelles cannot form after solvent annealing, as indicated in the experiment performed on the flat substrates. In the trough, highly ordered PS-*b*-P4VP micelle arrays were seen, as shown in Figure 3d.

Influence of Vapor Pressure on the Surface Morphologies of PS-*b*-P4VP. We investigated the effect of vapor pressure on the surface morphologies of PS-*b*-P4VP thin films. According to well-known Le Chatelier's principle,[38] increasing the temperature of a system increases the amount of vapor present, and so the saturated vapor pressure increases. Temperature was controlled by putting a small vessel in an oil bath. Figure 4 shows the SFM images of the films annealed at different temperatures for 10 min. When the films were annealed at 30 °C for 10 min, an increase of only 7 °C, it was dramatically developed as shown in Figure 4b. It is similar to that of a sample annealed at 23 °C for 1 h. In the case of film annealed at 40 °C, it seems that the lateral order of micelles is similar to that of a sample annealed at 23 °C for 2 h (Figure 4c). Contrary to increasing vapor pressure, an additional pressure was applied to the small vessel using argon gas. Even though the films are annealed at 23 °C for 1 h under additional pressure (1 psi), it was not developed due to lower vapor pressure as shown in Figure 4d. It should be noted that the vapor pressure in the system plays an important role in developing the micelle structure.

We extended to systems having different grating intervals. Figure 5a shows a phase mode SFM image obtained from a grating pattern having 2.5 μm interval and a line width of 80 nm. After annealing, one can see that topographic patterns are efficient in promoting long-range ordering of the PS-*b*-P4VP micelles, even though the grating interval increases. Near the grating pattern, a similar micelle array was

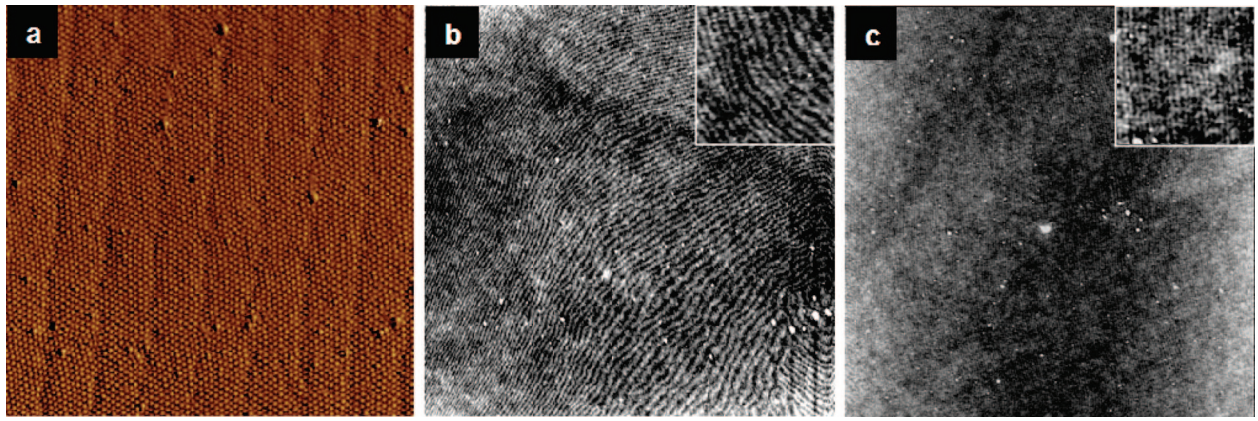

Figure 6. Micellar structure and Moiré pattern of PS-*b*-P4VP films annealed in THF vapor for 8 h on the grating pattern having shallow depth: (a) phase mode SFM images of micelles (2 μm × 2 μm), Moiré patterns (20 μm × 20 μm) obtained from SFM scan in the unpatterned (b) and patterned regions (c). In the inset, micelle arrays with the high degree of lateral order are shown on patterned regions, while different grains and bending of micelle arrays are seen on unpatterned regions.

observed (Figure 5b), with micelle arrays along with troughs located at the outside of the patterns. The lateral order of both regions is good within the scanning range of 5 μm × 5 μm. However, in the larger scanning size, significant difference was seen as will be mentioned later. The Fourier transform of the SFM image is shown in the insets of Figure 5a,b, where six-point patterns are seen, which is characteristic of the long-range ordered hexagonal array. From these results, we expect that the PS-*b*-P4VP micelle system can be used to obtain highly ordered arrays, regardless of grating pattern size and interval. In addition to grating patterns having shallow depth, we used a trench pattern (Seagate) having a depth of ~75 nm and a trench width of ~420 nm to develop the micelles. After solvent annealing for 6 h, a behavior similar to that of the grating pattern used in this study was seen (see Supporting Information, Figure S6). The micellar size on the mesa increases due to dewetting, while the well-developed micellar structure was seen in the trench regions. The method used in this study can be applied to any system to get long-range ordered micelles. From the results obtained on grating and trench patterns, we can conclude that PS-*b*-P4VP micellar arrays are reorganized into the hexagonal array with a high dregree of long-range lateral order both within and outside the pattern simultaneously during solvent annealing in THF vapor. Micellar arrays can be guided by the grating or trench patterns, while the arrays of micelles are not guided in the unpatterned regions.

To investigate the effect of grating patterns on the lateral of order of micelles, we have used the grating patterns having the crest-to-trough depth of ~5 nm. In the case of this pattern after solvent annealing, the dewetting phenomena were not seen, as shown in Figure 6a, and we could obtain the Moiré patterns to characterize the order and orientation of micelles in the wide range between the inside and outside patterns. Moiré patterns are formed from interference between a reference and a sample grating. Under certain conditions, one can observe the grain size, shape, orientation, and dislocation directly, as reported by Hexemer *et al.*[23] The Moiré pattern analyses were performed as a function of the solvent annealing time in THF vapor with unpatterned substrates. As the annealing time increases, a significant increase in the grain size was found (see Supporting Information, Figure S7). After solvent annealing for 6 h in THF vapor, a single grain size of at least 5 μm × 5 μm was obtained. For clarity, the Moiré patterns obtained from the 10 μm × 10 μm are not shown and only those from 5 μm × 5 μm SFM images are shown. We compared the Moiré pattern obtained from PS-*b*-P4VP films developed on unpatterned substrates with that on patterned ones. Figure 6b,c shows the Moiré patterns of unpatterned and patterned regions obtained from the SFM scan, respectively. In the patterned regions, the micelles are oriented uniaxially within a scan range of 20 μm × 20 μm, while multigrains are seen in the unpatterned regions. In the inset, micelle arrays with the high degree of lateral order were shown on patterned regions, while different grains and bending of micelle arrays were seen on unpatterned regions.

CONCLUSIONS

We have demonstrated a route for preparing the high-quality patterned micelle arrays using the PS-*b*-P4VP copolymer. Topographic patterns including grating and trench patterns are efficient in promoting long-range order of PS-*b*-P4VP micelles during solvent annealing in THF vapor. By controlling the line widths of grating patterns, we prepared micelle arrays of different sizes on the crests and in the troughs of the patterned surface. These arrays can be used as templates for pattern transfer to the underlying substrates or as scaffolds for the preparation of highly ordered quantum dot arrays.

EXPERIMENTAL SECTION

Materials. Poly(styrene-*b*-4-vinylpyridine) (PS-*b*-P4VP) sample was purchased from Polymer Source and was used without further purification (M_n,PS = 47.6 kg/mol, M_n,P4VP = 20.9 kg/mol, M_w/M_n = 1.14). PS-*b*-PVP copolymers were dissolved in *N*,*N*′-dimethylformamide (DMF, Fisher) at room temperature for 12 h to yield a 1.2 wt % polymer solution. The polymer solutions were prefiltered several times through Millipore 0.45 μm PTFE filters. PS-*b*-PVP thin films were fabricated by spin coating typically at 2500 rpm and 60 s from a 1.2 wt % DMF solution on the silicon substrate (International Wafer Source, Inc.) and cleaned in sulfuric acid and an inorganic oxidizing bath. The films were exposed to tetrahydrofuran (THF, Fisher) vapor for 5 min to 8 h to induce mobility. To control the solvent vapor treatment process, the samples were kept at a constant temperature (23, 30, and 40 °C) in a small closed vessel.

Preparation of Grating Pattern. Electron-beam lithography (JEOL 6400 SEM) was used to expose a 100 nm thick film of poly(methyl methacrylate) (spin coated from PMMA solution of 2% in anisole (Microchem Corp.) and baked at 170 °C in a gravity convection oven to improve adhesion), on oxidized silicon wafers. The single line exposures ranged from 0.3 to 7 nC/cm, which gave different line widths. Development in methyl isobutyl ketone/isopropyl alcohol (1/3, v/v) of the exposed pattern at room temperature for a minute and a rinse in isopropyl alcohol creates troughs with vertical side walls, and the evaporation of 14 and 5 nm thick silicon oxide *via* thermal evaporation on the developed region resembles oxidized silicon. This process is followed by acetone lift-off. One-dimensional troughs of various widths were used to study the array of block copolymer micelles.

Characterization of PS-*b*-P4VP Thin Films. The surface topography of PS-*b*-P4VP thin films on a silicon wafer was imaged by a scanning force microscope (Digital Instruments, Nanoscope III) in the tapping mode. The film thickness was measured by ellipsometry.

Acknowledgment. This work was supported by the U.S. Department of Energy, the NSF supported MRSEC and NSEC at the University of Massachusetts Amherst, and S.P. was supported by the Korea Research Foundation Grant funded by the Korean Government (KRF-2006-214-D00047).

Supporting Information Available: Characterization of grating pattern, the crest-to-trough depth of polymer surface, and development of block copolymer thin films on trench pattern. This material is available free of charge *via* the Internet at http://pubs.acs.org.

REFERENCES AND NOTES

1. Konodo, Y.; Takayanag, K. Synthesis and Characterization of Helical Multi-Shell Gold Nanowires. *Science* **2000**, *289*, 606–608.
2. Alivisatos, A. P. Semiconductor Clusters, Nanocrystals, and Quantum Dots. *Science* **1996**, *271*, 933–937.
3. Ashoori, R. C. Electrons in Artificial Atoms. *Nature* **1996**, *379*, 413–419.
4. Morales, A. M.; Lieber, C. M. A Laser Ablation Method for the Synthesis of Crystalline Semiconductor Nanowires. *Science* **1998**, *279*, 208–211.
5. Patzke, G. R.; Krumeich, F.; Nesper, R. Oxidic Nanotubes and Nanorods—Anisotropic Modules for a Future Nanotechnology. *Angew. Chem., Int. Ed.* **2002**, *41*, 2446–2461.
6. Fredrickson, G. H.; Bates, F. S. Dynamics of Block Copolymers: Theory and Experiment. *Annu. Rev. Mater. Sci.* **1996**, *26*, 501–550.
7. Bates, F. S.; Fredrickson, G. H. Block Copolymers—Designer Soft Materials. *Phys. Today* **1999**, *52*, 32–38.
8. Muthukumar, M.; Ober, C. K.; Thomas, E. L. Competing Interactions and Levels of Ordering in Self-Organizing Polymeric Materials. *Science* **1997**, *277*, 1225–1232.
9. Lazzari, M.; Lopez-Quintela, M. A. Block Copolymers as a Tool for Nanomaterial Fabrication. *Adv. Mater.* **2003**, *15*, 1583–1594.
10. Hamley, I. W. Nanotechnology with Soft Materials. *Angew. Chem., Int. Ed.* **2003**, *42*, 1692–1712.
11. Förster, S.; Antonietti, M. Amphiphilic Block Copolymers in Structure-Controlled Nanomaterial Hybrids. *Adv. Mater.* **1998**, *10*, 195–217.
12. Thurn-Albrecht, T.; Schotter, J.; Kästale, A.; Emley, N.; Shibauchi, T.; Krusin-Elbaum, L.; Guarini, K.; Black, C. T.; Tuominen, M. T.; Russell, T. P. Ultrahigh-Density Nanowire Arrays Grown in Self-Assembled Diblock Copolymer Templates. *Science* **2000**, *290*, 2126–2129.
13. Lopes, W. A.; Jaeger, H. M. Hierarchical Self-Assembly of Metal Nanostructures on Diblock Copolymer Scaffolds. *Nature* **2001**, *414*, 735–738.
14. Ross, F. M.; Kammler, M.; Reuter, M. C.; Hull, R. *In-situ* Observations of Self-Assembled Island Nucleation on Patterned Substrates. *Philos. Mag.* **2004**, *84*, 2687–2697.
15. Xia, Y.; Yin, Y.; Lu, Y.; McLellan, J. Template-Assisted Self-Assembly of Spherical Colloids into Complex and Controllable Structures. *Adv. Funct. Mater.* **2003**, *13*, 907–918.
16. Naito, K.; Hieda, H.; Sakurai, M.; Kamata, Y.; Asakawa, K. 2.5-Inch Disk Patterned Media Prepared by an Artificially Assisted Self-Assembling Method. *IEEE Trans. Magn.* **2002**, *38*, 1949–1951.
17. Segalman, R. A.; Hexemer, A.; Kramer, E. J. Effects of Lateral Confinement on Order in Spherical Domain Block Copolymer Thin Films. *Macromolecules* **2003**, *36*, 6831–6839.
18. Cheng, J. Y.; Ross, C. A.; Thomas, E. L.; Smith, H. I.; Vancso, G. J. Templated Self-Assembly of Block Copolymers: Effect of Substrate Topography. *Adv. Mater.* **2003**, *15*, 1599–1602.
19. Stoykovich, M. P.; Müller, M.; Kim, S. O.; Solak, H. H.; Edwards, E. W.; de Pablo, J. J.; Nealey, P. F. Directed Assembly of Block Copolymer Blends into Nonregular Device-Oriented Structures. *Science* **2005**, *308*, 1442–1446.
20. Cheng, J. Y.; Mayes, A. M.; Ross, C. A. Nanostructure Engineering by Templated Self-Assembly of Block Copolymers. *Nat. Mater.* **2004**, *3*, 823–828.
21. Li, H.; Huck, W. T. S. Ordered Block-Copolymer Assembly Using Nanoimprint Lithography. *Nano Lett.* **2004**, *4*, 1633–1636.
22. Sundrani, D.; Darling, S. B.; Sibener, S. J. Guiding Polymers to Perfection: Macroscopic Alignment of Nanoscale Domains. *Nano Lett.* **2004**, *4*, 273–276.
23. Hexemer, A.; Stein, G. E.; Kramer, E. J.; Magonov, S. Block Copolymer Monolayer Structure Measured with Scanning Force Microscopy Moire Patterns. *Macromolecules* **2005**, *38*, 7083–7089.
24. Xiao, S.; Yang, X.; Edwards, E. W.; La, Y.-H.; Nealey, P. F. Graphoepitaxy of Cylinder-Forming Block Copolymers for Use as Templates to Pattern Magnetic Metal Dot Arrays. *Nanotechnology* **2005**, *16*, S324–S329.
25. Chai, J.; Wang, D.; Fan, X.; Buriak, J. M. Assembly of Aligned Linear Metallic Patterns on Silicon. *Nat. Nanotechnol.* **2007**, *2*, 500–506.
26. Yoon, B.; Huh, J.; Ito, H.; Frommer, J.; Sohn, B. -H.; Kim, J. H.; Thomas, E. L.; Park, C.; Kim, H. -C. Smart Self-Adjustment of Surface Micelles of an Amphiphilic Block Copolymer to Nanoscopic Pattern Boundaries. *Adv. Mater.* **2007**, *19*, 3342–3348.
27. Riess, G. Micellization of Block Copolymers. *Prog. Polym. Sci.* **2003**, *28*, 1107–1170.
28. Moffitt, M.; Khougaz, K.; Eisenberg, A. Micellization of Ionic Block Copolymers. *Acc. Chem. Res.* **1996**, *29*, 95–102.
29. Xuan, Y.; Peng, J.; Cui, L.; Wang, H.; Li, B.; Han, Y. Morphology Development of Ultrathin Symmetric Diblock Copolymer Film *via* Solvent Vapor Treatment. *Macromolecules* **2004**, *37*, 7301–7307.
30. Zhao, J. C.; Jiang, S. C.; Ji, X. L.; An, L. J.; Jiang, B. Z. Study of the Time Evolution of the Surface Morphology of Thin Asymmetric Diblock Copolymer Films under Solvent Vapor. *Polymer* **2005**, *46*, 6513–6521.

31. Yun, S.-H.; Yoo, S. I.; Jung, J. C.; Zin, W.-C.; Sohn, B.-H. Highly Ordered Arrays of Nanoparticles in Large Areas from Diblock Copolymer Micelles in Hexagonal Self-Assembly. *Chem. Mater.* **2006**, *18*, 5646–5648.
32. Andelman, D.; Joanny, J.-F.; Robbins, M. O. Complete Wetting on Rough Surfaces: Statics. *Europhys. Lett.* **1988**, *7*, 731–736.
33. Robbins, M. O.; Andelman, D.; Joanny, J.-F. Thin Liquid Films on Rough or Heterogeneous Solids. *Phys. Rev. A* **1991**, *43*, 4344–4354.
34. Li, Z.; Tolan, M.; Höhr, T.; Kharas, D.; Qu, S.; Sokolov, J.; Rafailovich, M. H.; Lorenz, H.; Kotthaus, J. P.; Wang, J.; Sinha, S. K.; Gilbaud, A. Polymer Thin Films on Patterned Si Surfaces. *Macromolecules* **1998**, *31*, 1915–1920.
35. Rehse, N.; Wang, C.; Hund, M.; Geoghegan, M.; Magerle, R.; Krausch, G. Stability of Thin Polymer Films on a Corrugated Substrate. *Eur. Phys. J. E* **2001**, *4*, 69–76.
36. Spatz, J. P.; Möller, M.; Noeske, M.; Behm, R. J.; Pietralla, M. Nanomosaic Surfaces by Lateral Phase-Separation of a Diblock Copolymer. *Macromolecules* **1997**, *30*, 3874–3880.
37. Krishnamoorthy, S.; Pugin, R.; Brugger, J.; Heinzelmann, H.; Hinderling, C. Tuning the Dimensions and Periodicities of Nanostructures Starting from the Same Polystyrene-*block*-Poly(2-vinylpyridine) Diblock Copolymer. *Adv. Funct. Mater.* **2006**, *16*, 1469–1475.
38. Atkins, P. W. *Physical Chemistry*, 6th ed.; Oxford University Press: Oxford, 1998.